Ray
Bernie
Brent
Don
Grant
JR
Joe D
Stu

Ian
Rolly

- use CSI 2110 + clip on CT
- Auto range
- 3200 line resolution
- 0 - 400 Hz Span
- Logarithmic scale (db).

Stu

GE Industrial & Power Systems

Broken Bar Detector For Squirrel Cage Induction Motors

G.B. Kliman and A.V. Mohan Rao
GE Company
Schenectady, New York

Broken Bar Detector
For Squirrel Cage Induction Motors

by

G. B. Kliman
General Electric Company
Corporate Research & Development
Schenectady, NY

A. V. Mohan Rao
General Electric Company
Industry Service Engineering
Schenectady, NY

ABSTRACT

Several of the leading theoretical developments describing the behavior of squirrel cage induction motors with faulted cages are reviewed. Key features of these and other developments are used to develop a flexible computer based instrument which processes motor current data to derive information concerning the integrity of the rotor cage. Such an instrument was built and tested in the laboratory on an inside-out motor with various faults imposed on it. The instrument was then sent into the field for unassisted trials at various power plants with good results. The PC based instrument is now commercially available through the General Electric Company.

INTRODUCTION

Recent statistical data [1] concerning failures among utility size induction motors indicate that at least 10% of the failures are rotor related and half of these are due to faults in the cage. Field experience suggests that the incidence of broken rotor bars is actually much higher. Complicating this problem has been the difficulty of determining that there indeed is a broken bar and not another problem having similar symptoms such as excessive vibration or noise and sparking during starting. Such symptoms will usually be evident only when several bars have been broken in any case. Often a motor will be sent out repeatedly for balancing in an attempt to remedy a potential cause of vibrations, when the cause of the vibrations is really due to the presence of broken bars.

In the past, tests designed for use in the shop or when the motor is shut down, have been only partly satisfactory. The need for a more sensitive testing method was recognized and it was evident that an "on-line" monitor should be used. A number of studies were directed toward developing such an "on-line" system. Typical of these were the theoretical papers of Williamson [2] and Deleroi [3]. The first such on line monitor to be developed and used was the shaft oscillation detector of Gaydon [4].

The development work reported in this paper was started in 1984 under the sponsorship of the Electric Power Research Institute. The resulting detector has the sensitivity to detect the presence of a single broken bar or an open end ring. Test results suggest that even cracks or bad joints may be detectable. Three further requirements were imposed by the sponsor. These required the instrument to be:

1. Capable of operation (with less sensitivity) using only one test,
2. Operable, with little or no training, by the average instrumentation technician,
3. Non-invasive.

It was recognized, however, that the best application would be in a trending mode starting with a baseline test when the motor was in known good condition. A fourth requirement dictated that the system should have a sensitivity sufficient for discriminating the presence of a single broken bar and averting false alarms due to other rotor asymmetries.

II FAULT MODELING

When a rotor bar breaks, the current path in the cage will redistribute as shown in Fig. 1 where Fig. 1 (a) depicts the current distribution in an ideal cage. Fig. 1 (b) depicts the approximate redistribution of current when a single bar is completely severed. Most theories of motor performance with broken bars start with a ladder network approach (Fig. 2 [3]) to modeling a rotor

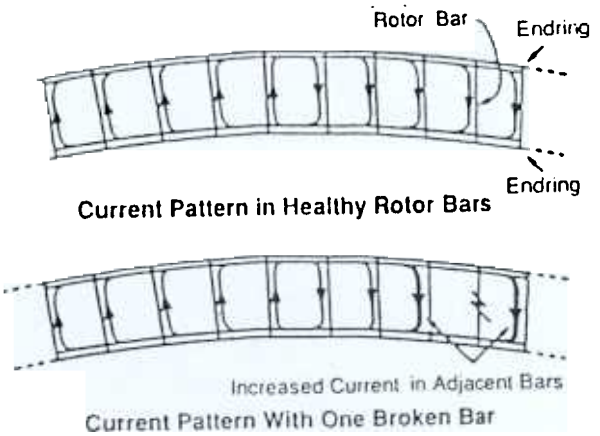

Fig - Current patterns in an induction motor rotor with (a) all bars healthy and (b) one broken bar.

similar to the one depicted in Fig. 1. In the ladder network approach (Fig 2.), each bar and end are assigned appropriate self inductances and resistances. Mutual effects are usually handled by calculating the resultant air-gap fields, in simplified geometry, based on assumed currents and solving for the self consistent currents. The break may be modeled by subtracting the symmetrical currents so that the broken bar is replaced by the current generator as shown.

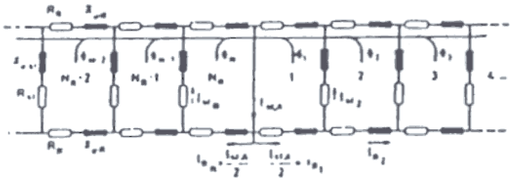

Fig. 2 - Ladder network model of a rotor cage with one broken bar.

The effect on steady state performance was calculated by Mavridis [5]. The current and full load slip are shown in Fig. 3 as a function of the number of bars broken per pole. It is immediately evident that the resultant performance modification would be difficult to measure in the laboratory and impossible to measure in the field. Torque pulsations would, however, be quite large (Fig. 4) and the resulting speed oscillations may be used to imply the presence of a broken bars if the net inertia is not too large [4]. Williamson [2] used a detailed circuit model to find the redistribution of the currents in a broken bar rotor. An example of these calculations is given in Fig. 5 where the large increase in losses in bars adjacent to the break is strikingly illustrated. Deleroi [3] used a similar but much simplified model which neglected the stator windings. Such features as the asymmetry were lost but the closed form results were adequate for use in this study and convenient for examining large numbers of motor designs. In contrast Elkasagbi [6] carried out a series of highly detailed finite element method studies (Figs. 6 & 7) which verified that the prior work was valid at low and normal slip but not at high slip.

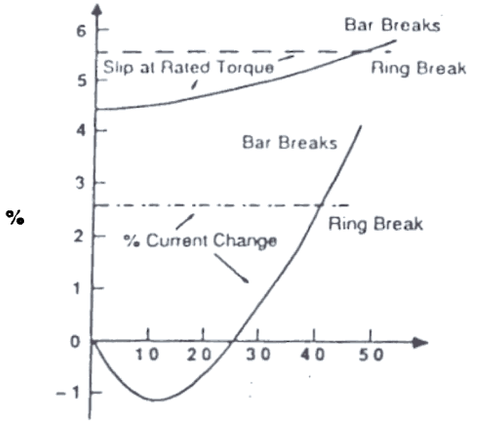

No. of Bars Broken in % of the No. of Bars/Pole

Fig. 3 - Effect of broken bars on steady state (fundamental) performance.

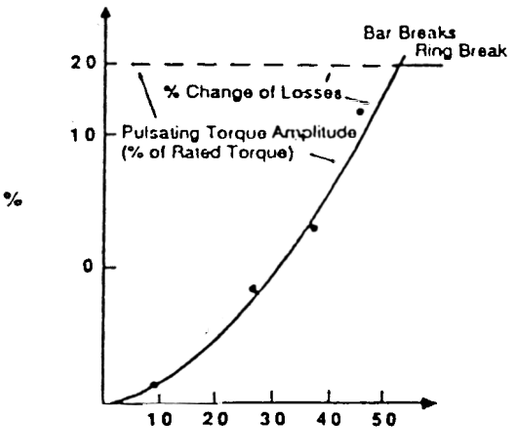

No. of Bars Broken in % of No. of Bars/Pole

Fig. 4 - Effect of broken bars on torque pulsations.

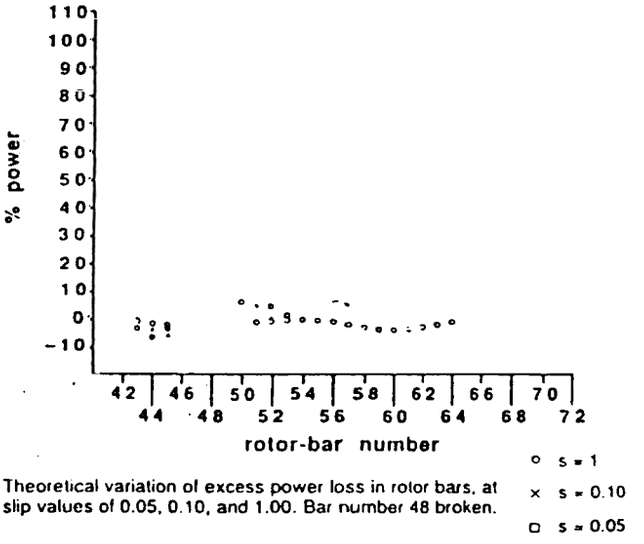

Theoretical variation of excess power loss in rotor bars, at slip values of 0.05, 0.10, and 1.00. Bar number 48 broken.

Fig. 5 Prediction of power loss in bars adjacent to break.

Fig. 6 - The field distribution at full load (1760 rpm).
(a) no broken bars (b) five broken bars

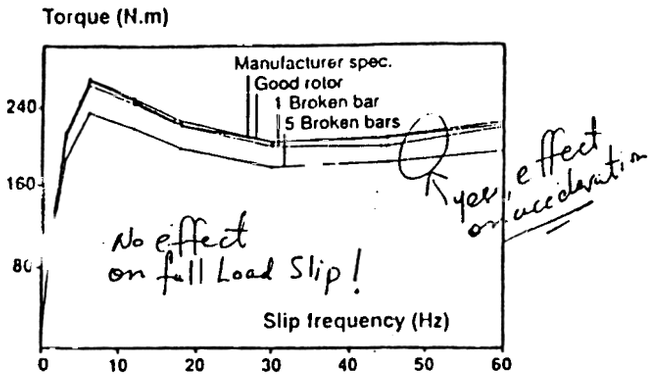

Fig Computed torque-slip frequency characteristics for the 30 hp induction motor with zero, one, and five broken bars.

The simplified theory [3] may be used to illustrate the nature of the air-gap fields in the presence of a bar break. Fig. 8 shows how the air-gap flux density phasors of the fault disturbance vary around the rotor. The real and imaginary components of the phasor are depicted in planes arranged perpendicular to the azimuthal direction in a coordinate system fixed to the rotor. It may be seen that the magnitude diminishes and phase increases as the distance from the break increases. Directly over the break there is an abrupt reversal of the field sometimes described as a swirl. The field anomaly rotates at the mechanical speed of the rotor since it is fixed to the broken bar. The rotating flux and current are pulsating at slip frequency. The flux distribution may be resolved into a series of counter-rotating slip frequency waves of decreasing wavelength on the rotor as seen from the stator. Note that the fundamental of these waves is always two pole regardless of the number of poles on the stator.

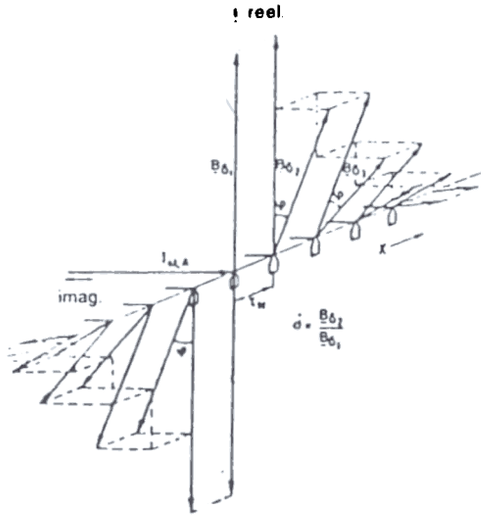

Fig. 8 Phasors of air-gap flux density along a broken bar rotor cage.

When the counter-rotating waves are transformed to the stationary frame the space harmonics become time harmonics. Fig. 9 shows the spectrum of the air-gap flux density at one point in the stationary frame for a typical 2500 HP, 900 RPM gas recirculation fan motor with one broken bar. Note that each line is actually two lines separated by twice the slip frequency (60s) but not resolved on the printer at this scale. The actual frequencies are given by

$$f_k = f_0 [(k/p)(1-s) \pm s]$$

where
- f = line frequency (usually 60 Hz)
- k = harmonic index ($k = 1, 2, 3, \ldots$)
- p = number of pole pairs
- s = per unit slip

All of these frequencies will be present in the air-gap flux. The spectrum shape shown in Fig. 9 is controlled by the rotor parameters combined into the "cage magnetic Reynolds number" or "motor goodness factor". The shape does not vary a great deal for most large power plant motors. When the winding pitch and distribution factors are applied and the line current calculated the spectrum of Fig. 10 is obtained. The pole pitch of the winding must also be taken into account which removes all but the checked lines i.e., the "normal" harmonics except that the "broken bar" lines appear at displaced frequencies given by equation (1). Due to manufacturing tolerances other frequencies may not exactly cancel out and may be measurable but of unpredictable amplitude. The major harmonics will be predictable and reproducible and form the basis of the motor "personality" used in the instrument. The magnitude of the fundamental component for a single broken bar will, typically, be about 35 to 45 db below the 60 Hz power component of current compared to residual magnitudes typically 60 db below the 60 Hz component for good motors.

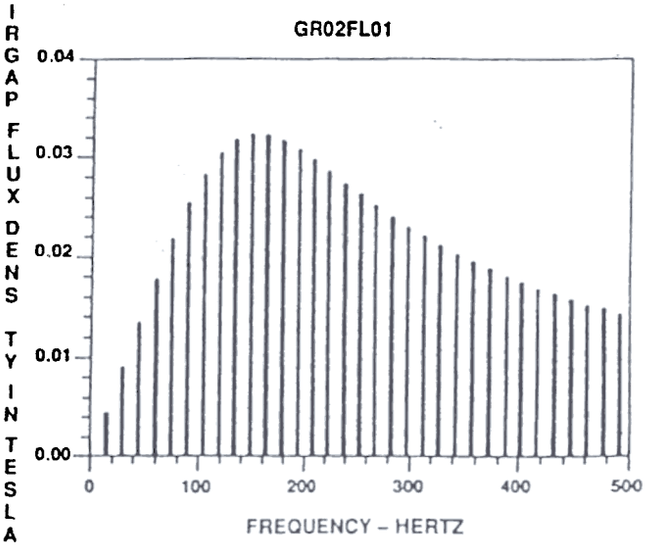

Fig. 9 Air-gap flux spectrum as seen from the stator of an 8-pole gas recirculation fan with one broken bar.

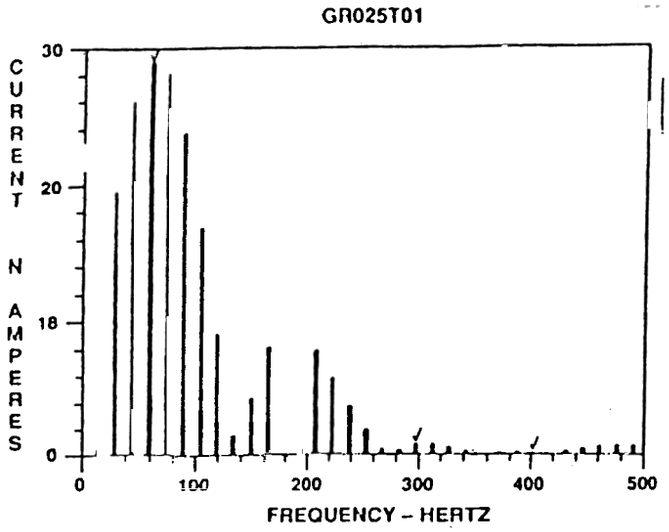

Fig. 10 Predicted line current for a single broken bar (based on Fig. 8) with pitch and distribution factors and inductance applied. Only the checked harmonics are predicted to be present.

As previously mentioned, when the sensitivity is high enough to detect the presence of a single broken bar other rotor asymmetries may cause confusion and false alarms. A brief study [7] was carried out to estimate the magnitude of the likely interfering effects. A comparison of the first few air-gap harmonics for these effects with those for a single broken bar in a typical motor is shown in Fig. 11. Note that there is a real possibility of mistaking the effects of a rotating eccentricity (bearing whirl) or an out of round rotor for a broken bar especially for two pole machines. The case of magnetic anisotropy shown is for an extreme situation which is unlikely to be seen in practice. Fig. 11 also suggests the way in which such ambiguity may be resolved. It is easily seen that the harmonics of a broken bar are much greater than

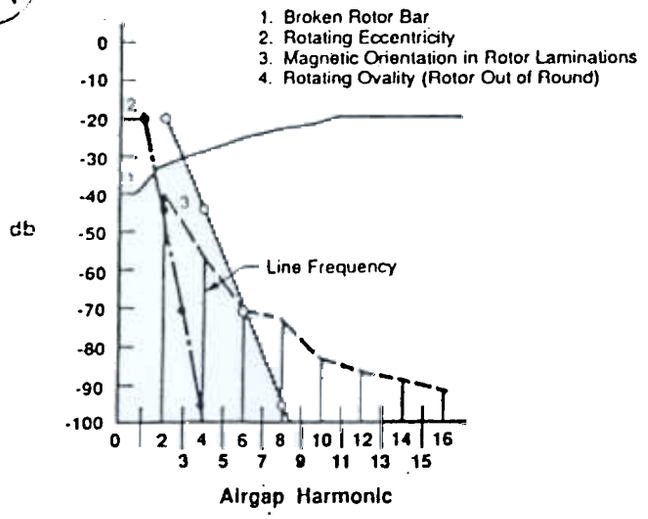

ig 11 Comparison of air-gap flux spectra for a single broken bar with various asymmetries in a typical 4 pole motor.

for an asymmetry and this property is used to differentiate the cases. In situations where there is more than one bar broken this feature will rarely be needed due to the unmistakable size of the signal.

III. CONTROLLED EXPERIMENTS

A series of exploratory experiments were carried out on a heavily instrumented, 50 HP, 1800 RPM motor of standard design to verify the major aspects of the theory, and to examine various possible indicators and other methods of detection. Among the results of this part of the study were the developments of a simplified FM demodulation device to implement a low cost shaft oscillation detector and an ensemble averaging system applied to an air-gap flux sensor. The latter instrument was sensitive enough to map the conductivity variations of the bars due to casting nonuniformities and included the capability of locating the faulty bar on the rotor. All three approaches have been reported elsewhere [8], [9] and patented (2 granted, 1 pending).

The major database underlying the instrument calibration was obtained from two sources:

(1) A series of detailed tests run on a 35 HP, 6 pole inside-out motor, which was designed to simulate the characteristics of a large power plant motor.

(2) A number of motor tests, on-site and at various power plants to obtain realistic field data.

In the on-site tests one motor was found to have a broken bar previously unsuspected by plant personnel.

The use of an overhung, bar wound, inside-out motor allowed various kinds of fault conditions to be conveniently and safely tried on an operating motor. Baseline tests were run with a healthy cage and uniform air-gap. Subsequently the nominal 60 mil air-gap was offset by 10 mils in the vertical direction by shimming the bearings to simulate a rotational asymmetry. One 1.25 inch high bar was then partially cut 3/4, 7/8 and fully through to test whether the chosen approach could distinguish between cracked and fully broken bars. Following that additional bars were cut through to measure the effect of two and three adjacent broken bars. Two of the bars were then repaired and another bar on the opposite side of the rotor was cut through.

Following the broken bar tests all of the cut bars were repaired and the end ring cut. Surprisingly the motor started and ran normally with the cut end ring. The apparent reason for this is the bar-to-lamination contact allowing rotor currents to flow in the laminations thus diluting the effect of the break [10].

The test series included measurement of line current, air-gap flux density and external stray flux. This paper will deal only with line current spectra but the detailed results including air-gap and external flux may be found in the complete report [11].

IV THE COMPUTER BASED INSTRUMENT

The instrument performs two major functions: signal processing and implementation of the decision algorithms. A long time interval sample of the current is acquired digitally in the form of an array of numbers representing the magnitude of the current at closely spaced times. The sampling time must be long enough, in this case about 30 seconds, to yield the desired resolution in frequency, about 0.03 Hz, in order to distinguish signals separated by twice the slip frequency which may be as low as 0.3 Hz in large power plant motors. The sample spacing must be close enough to encompass all of the harmonics of the line frequency to be examined. In the case of the developmental instrument the range was extended through the 13th harmonic of 60 Hz or 780 Hz which then required a sampling frequency of about 1850 Hz.

After the digital sample is acquired it is transformed using the Fast Fourier Transform (FFT) into a spectrum which is then searched for the particular harmonics, given by Equation (1), characteristic of broken bars. The resulting set of harmonic amplitudes is the broken bar "personality" of the motor. The required resolution and bandwidth demand an FFT size of 64K points.

In order to capture this data automatically, instead of as it is usually done by visual inspection of the spectra, it is necessary to know the line and slip frequencies to a high degree of precision. Line frequency may be obtained from the current but slip frequency is normally derived from the speed. Fortunately a non-invasive method of measuring slip frequency directly in the external axial leakage flux has been developed [12] and is used here. A simple round coil is mounted, coaxial to the shaft on the outside of the case. When the signal from this coil is analyzed in the same manner as the current a strong spectral component at slip frequency appears. Once the slip and line frequencies are known the motor "personality" may be extracted. To gain the maximum precision, the external axial flux and the current are measured at the same time by interleaving data samples.

A functional block diagram of the instrument is shown in Fig. 13 The software is designed so that the spectra, from which the motor personalities are derived, may be viewed at the option of the operator. Fig. 14 is a set of such spectra in the vicinity of 60 Hz for zero, one two and three broken bars. The predicted position of the broken bar spectral line is indicated by a dashed line placed by the software. The characteristic frequencies are 60 Hz and 60(1-2s). The 60 Hz component is swallowed up in the power component. The component visible at 60(1+2s) is due to the speed oscillation induced by the low inertia test stand. Note also that the general noise level rises as bars are broken, thereby partially masking some of the increase in signal. Notice that other side bands appear especially for the case of three broken bars. Additional sidebands separated by multiples of 2s60 Hz will sometimes

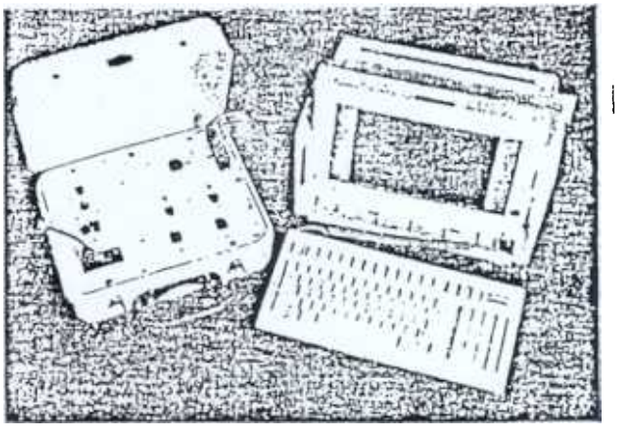

Fig. 12 - First commercialized version of the broken bar detector. (Photograph)

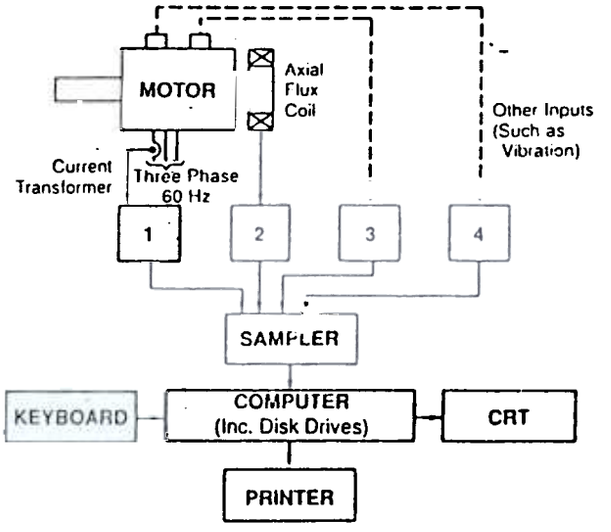

Fig. 13 - Broken bar detector functional block diagram.

appear due to harmonic currents flowing in the windings, from slots, phase belts and broken bars interacting with the rotor fault [13]. In this case the sidebands were not at such a frequency and were ultimately traced to a faulty coupling in the motor-generator set driving the test motor dynamometer loop. Fig. 15 shows an example of harmonic sidebands for the same conditions as Fig. 14.

Fig. 16 summarizes the results of the inside-out motor tests for the first and fifth harmonics. The variation of the harmonics with severity of break is much as predicted by theory except for one point in one of the 5th harmonic sidebands. This point was repeatable and is, at present, not explained as were some other minor variations. Again, as predicted, the natural or usual 5th harmonic was unaffected by the presence of faults and this pattern carried through the remaining harmonics.

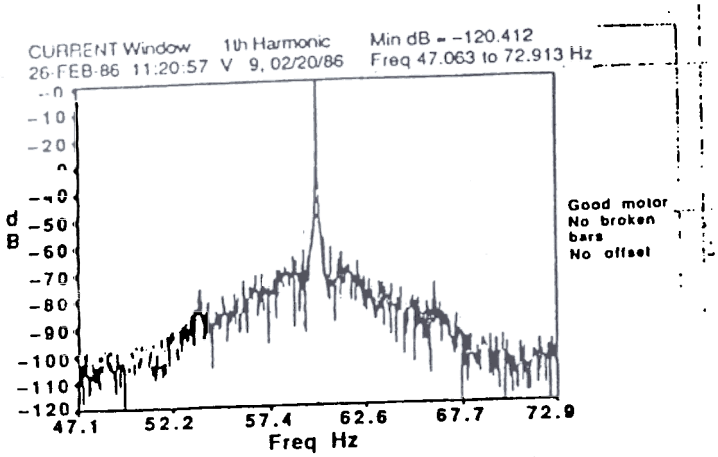

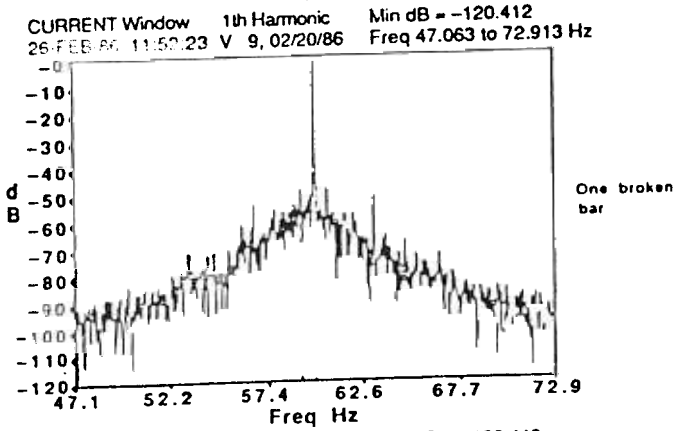

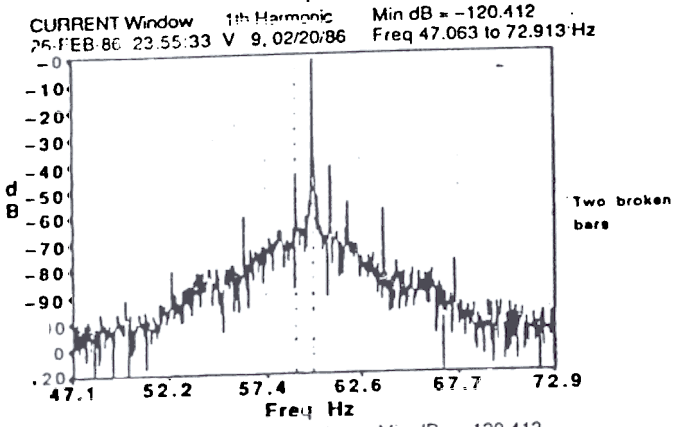

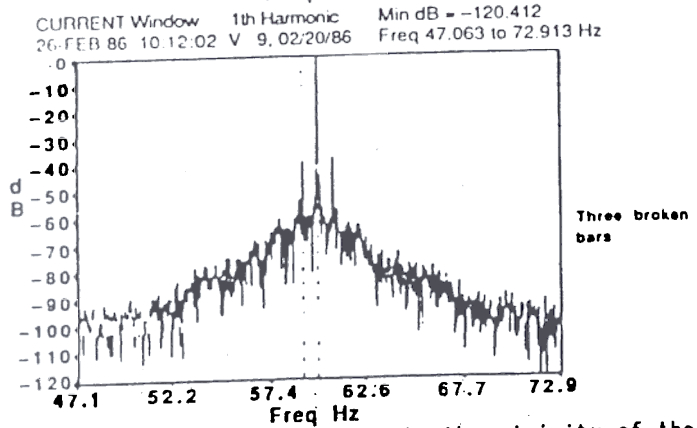

Fig. 14 Current spectra in the vicinity of the fundamental (60 Hz) for several increasingly severe rotor faults.

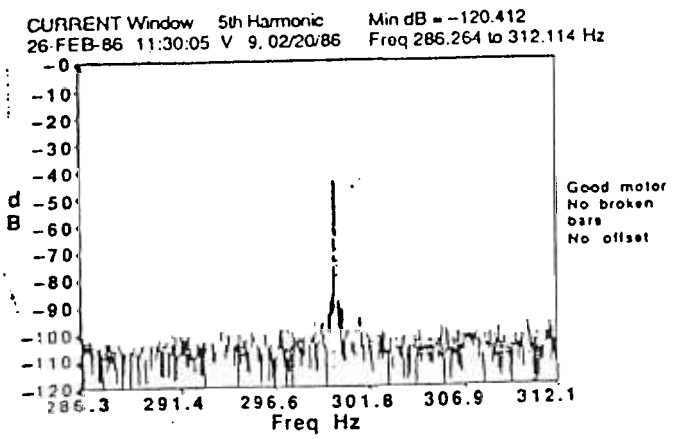

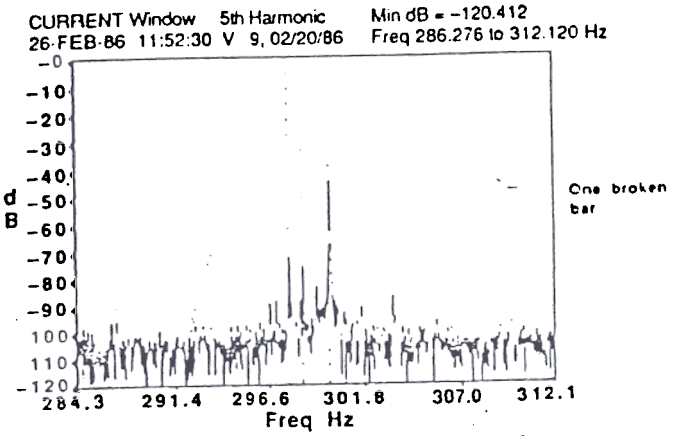

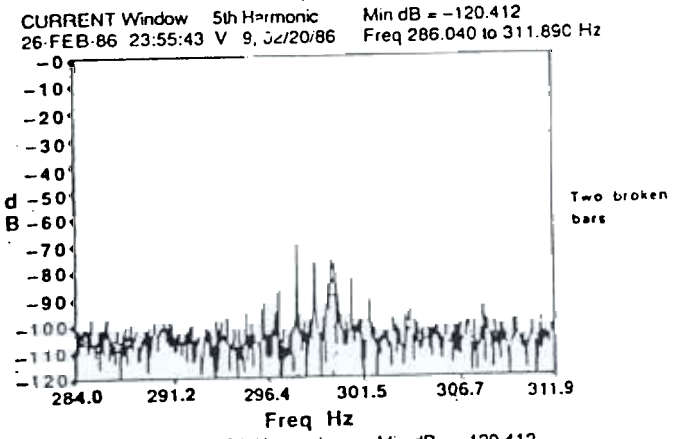

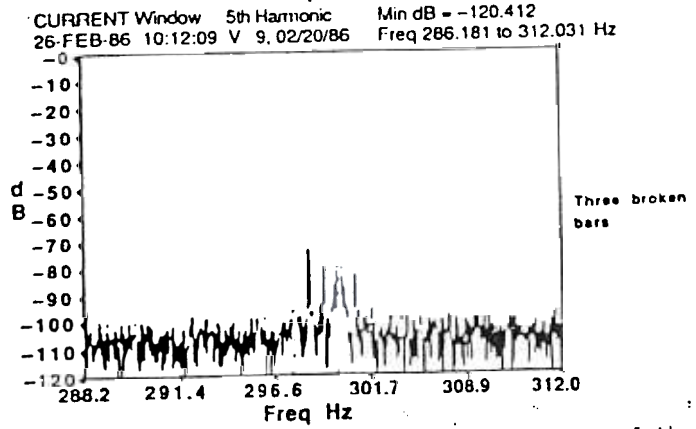

Fig 15 - Current spectra in the vicinity of the 5th harmonic for the conditions of Fig. 14.

FIELD TEST

The first round of field tests was carried out by R & D personnel in and around the GE plant in Schenectady and at a nearby facility of the Niagara Mohawk Power Corp. using the laboratory "breadboard" instrument. The results of these tests, for the 1st and 5th harmonics are shown in Fig. 16. All of the motors were, evidently, in good condition without broken bars and represented a variety of sizes, poles, windings and applications. It is remarkable and useful that the range of signals from them was, none the less, quite restricted (in db below the 60 Hz component) and provides the basis for "single look" decision making. All of the motors (ranging from 400 HP to 1200 HP) were running on the 60 Hz power line except 271 #1 which was powered by a square wave inverter. Points from the inside-out motor tests were included for comparison. It should be noted that the inverter 5th harmonic may have influenced the results to some extent but not more than the normal variation between motors.

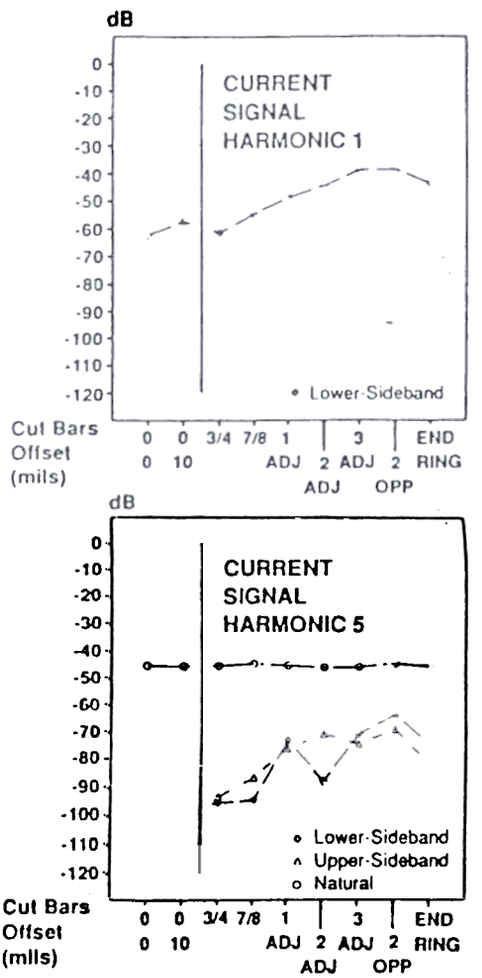

Fig. 16 - Summary of 1st and 5th current harmonics.

In a subsequent program the laboratory "breadboard" instrument along with the PDP-11 Computer was sent to a number of power plants across the US to gather field data under realistic conditions. No personnel from GE or EPRI accompanied the instrument nor were power plant personnel taken to Schenectady for training. After several months of field testing and evaluation, the instrument's software was rehosted to a "PC" compatible computer, Fig. 12. Results for the lower side band for the complete sample are shown in Fig. 17. Summary of the total field test data of the fundamental component is summarized in Figure 18.

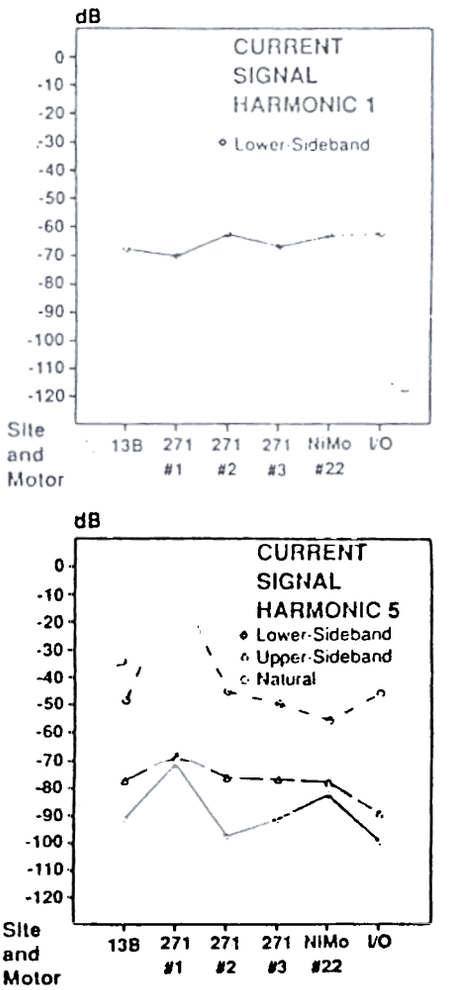

Fig. 17 - Summary of first round field test data for the 1st and 5th harmonics.

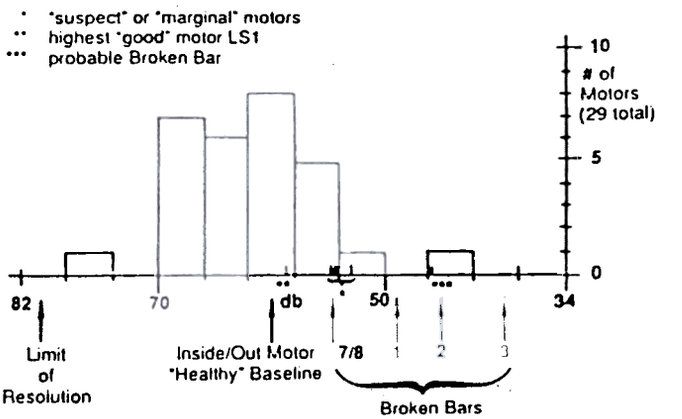

Fig. 18 Summary of total field test data of the fundamental component.

MOTOR TESTING USING THE "PC" BASED INSTRUMENT

To perform a test measurement, it is only necessary to use a clip-on current probe or transformer or insert a resistor into the secondary of the standard control center instrument or relay transformer to generate the current input signal. A multi-turn coil is hung outside the motor case, coaxial with the shaft, to sense slip frequency fluxes, caused by end ring currents, to enable detection of the slip frequency. These two quantities allow automatic determination of the "motor personality".

The instrument works by examination of the frequency spectrum of the line current. A normal motor will exhibit the familiar 5th, 7th, 11th, 13th, etc. harmonics due to the windings and non-linearities plus higher frequency slot related harmonics. The presence of a broken bar in the rotor causes a particular set of spectrum lines to appear in the current at frequencies distinct from the normal harmonics. These frequencies are uniquely given by a combination of slip and line frequencies. The Broken Bar Detector makes a record of current waveform and subjects it to Fourier analysis to develop the spectrum. By measuring the line and slip frequencies, the particular components relevant to broken bars may, automatically, be separated to form a "motor personality" which may then be numerically compared to a similar personality established when the motor was new or in known good condition. Preliminary criteria for different numbers of bars broken or asymmetry have been established for manual or automatic, simple indicator, operation.

To run the test, it is only necessary to operate the motor at full load (or as close to full load as is practical), start the operation of the detector software and follow the "on-screen" instructions. The detector hardware and software will automatically acquire the current and flux coil data, carry out the fast Fourier transform, select the appropriate spectral components to form the motor personality and decide the condition of the rotor. The operator's duties are to hook up the current and flux inputs, start the program and follow the instructions. The operator will first be instructed to gather and enter data copied from the nameplate and/or other data about the motor. Additional information identifying the motor, location, loading, speed, presumed problems, conditions surrounding or related to the test, operator, etc., will be entered at this time. Completeness of documentation is important, and it is better to have too much rather than too little.

The only other "set-up" functions required of the operator are to slowly vary the rough gain setting knobs on the current and flux amplifiers until the overload lights come on. At this point, the computer takes over operation, adjusts the gains to the optimum value and proceeds with the analysis of the data. Upon completion of the analysis, the computer will display the estimated condition of the rotor with one of the following messages:

No change from previous test.
2 Rotor is estimated to be OK.
3 There is probably a broken or cracked rotor bar.
4 There is at least one or, possibly, more broken bars.

Facilities are provided, within the software, for monitoring the inner details of the detector operation to assure that it is working properly and that the results being reported are reasonable. Guidelines for evaluating the operation are be provided in the manual and/or on screen. Experienced operators may want to examine the spectra to make their own evaluation, verify the programs's conclusions, check for other phenomena or check instrument operation. Again, guidelines for making manual or visual evaluations are also provided. The automatic features of the instrument are available to provide guidance in interpretation of the results.

VII. CONCLUSIONS

An EPRI sponsored research program has developed the basic data and a laboratory "breadboard" instrument for the detection of broken bars in induction motors. The instrument has been proven in field trials and has now been adopted by the General Electric Company for commercialization.

VIII ACKNOWLEDGMENTS

The initial development of the instrument was carried out under EPRI contract RP2331-1 directed by Jan Stein. Major participants in the GE team were E. L. Owen, R. A. Koegl, M. W. Schultz, S. E. Grabkowski, D. F. Lackey and J. J. Bockis. The original proposal for this work was written by E. Richter and T. J. Miller. The commercialization team has included J. A. Wolfinger, K. Rao and C. Wroblewski.

Field data trials have been conducted with the cooperation of Niagara-Mohawk Power Corp., Public Service Electric and Gas, Ohio Edison, Illinois Power, Tennessee Valley Authority, Georgia Power and Alabama Power.

IX REFERENCES

1. McCoy, R. M., et al, "Improved Motors for Utility Applications: Vol. I: Industry Assessment Study Update and Analysis". EPRI EL-4286, Vol. 1 (RP-1763-2), September 1985.

Williamson, S. and Smith, A. C., "Steady State Analysis of 3-Phase Cage Motors with Rotor Bar and End Ring Faults". IEEE Proc., Vol. 129, Pt. B, No. 3, May 1982, pp. 93-100.

3 Deleroi, W., Broken Bar in Squirrel-Cage Rotor of an Induction Motor, Part I: Description by Superimposed Fault Currents". Archiv fur Elektrotechnik 67, 1984, pp. 91-99.

4 Gaydon, B. G. and Tucker, C. F. J., "Detection of Rotor Defects in Induction Motors Using Minicomputer". CEGB Report SE/SSD/RN/80/074, Nov. 1980.

5. Mavridis, D., "On the Performance of Three Phase Squirrel Cage Induction Motors During the Presence of Bar or Ring Breaks." PhD Thesis, University of Hanover (Germany) 1963.

6. Elkasabgy, E. N., Eastham, A. R. and Dawson, G. E., "The Detection of Broken Bars in the Cage Rotor of an Induction Machine", IEEE-IAS, Annual Meeting, 1988, Pittsburgh, PA, pp. 181-187.

7. Richter, E., private communication.

8 Kliman, G. B. et al, "Non-invasive Detection of Broken Rotor Bars in Operating Induction Motors", IEEE-PES, Transactions on Energy Conversion. Vol. 3, No. 4, Dec., 1988.

9 Kliman, G. B., "Detection of Faulted Rotor Bars in Operating Induction Motors", International Conference on Electrical Machines, Munich, FRG, Sept., 1986.

10 Kerzenbaum, I. and Landy, C. F., "The Existence of Large Inter Bar Currents in Three Phase Squirrel Cage Motors With Rotor-Bar and/or End Ring Faults", IEEE, PAS-103, No. 7, July 1984, pp. 1854-1862.

11 Kliman, G. B. et al, "The Detection of Broken Bars in Motors", EPRI RP2331-1 (in print).

12 Erlicki, M. S., Porat, Y., and Alexandrovitz, A., "Leakage Field Changes of an Induction motor as Indication of Nonsymmetric Supply", IEEE Transaction IGA-7, No. 6, Nov./Dec, 1972, pp. 713-717.

13. Welsh, M. S., "Detection of Broken Rotor Bars in Induction Motors Using Stator Current Measurements", SM Thesis, MIT, Cambridge, Massachusetts, May, 1988.

For more information and quotations contact:

GE Industrial & Power Systems
A.V. Mohan Rao (518) 385-3564
Industry Services Engineering
Building 55, Room 257
Schenectady, N.Y. 12345

NOTICE

The technical discussions in this report was prepared by the GE Company. Neither the GE Company, nor any person acting on behalf of GE (a) makes any warranty or representation, express or implied, with respect to the accuracy, completeness, or usefulness of the information contained in this report, or (b) assumes any liabilities with respect to the use of, or for damages resulting from the use of, any information, apparatus, method, or process disclosed in this report.

When a permanent probe is purchased from GE, a contract describing limited liability will be agreed to with the customer.

GER-3609 6/89 (500)